Numerical Estimation of Crack Openings in Concrete Structures Under Multi-physic Loadings

François Soleilhet, Farid Benboudjema, Xavier Jourdain, and Fabrice Gatuingt

Abstract Cement based material structures are designed to work in pair with steel reinforcement. The cracking of reinforced concrete is a normal phenomenon given the working principle of this material. But, for aesthetic or durability reasons, the openings of these cracks must be controlled. In the modelling, there is often an ambiguity between damage (micro-cracking at the scale of a REV) and crack opening at the scale of the material. The goal of this study is to estimate the crack opening in concrete structures under various multi-physic loadings. To do so, a method based on continuum mechanics is developed. This method post-processes the mechanical damage induced by the diverse loadings. To illustrate the procedure, a numerical application is run on an experimental reinforced shear wall made of ordinary concrete submitted to drying prior to loading. A hygro-mechanical model previously developed by the authors is firstly calibrated on experimental data and secondly used to compute the shear wall's damage induced by drying shrinkage. The resulting computed crack openings are compared to the experimental results. Interestingly, the post-processing technique managed to locate the areas where cracks are of major importance. However, the assumption of perfect adhesion between concrete and steel leads to a slight underestimation of the amplitude of the crack opening. In a first attempt to capture cracks, the proposed method based on continuum mechanics seems to be a good alternative to sophisticated methods.

Keywords Concrete · Damage · Crack opening · Multi-physic loadings

F. Soleilhet (✉)
EDF R&D, Les Renardières, 77250 Ecuelles, France
e-mail: francois.soleilhet@edf.fr

F. Soleilhet · F. Benboudjema · X. Jourdain · F. Gatuingt
CNRS, LMT – Laboratoire de Mécanique et Technologie, Université Paris-Saclay, ENS Paris-Saclay, 91190 Gif-sur-Yvette, France

1 Introduction

Cementitious material are often used in pair with steel reinforcement. They are thus intended to crack. These cracks are of importance regarding durability issues. To control and maintain durability, design codes and standards give recommendations regarding crack opening.

Nowadays, the assessment of the mechanical state of structure is regularly obtained with numerical simulations. Different approaches with different levels of complexity are available to model concrete cracks [1]. To assess the mechanical state of a structure, damage modelling can be used. This method is affordable regarding calculation time and allows to model correctly the concrete failure process. However, the main drawback of this method is that it does not model explicitly the cracks and gives only information regarding diffuse micro-cracks with the damage index. To extract crack opening from damage model, post-processing technics were developed [2, 3]. Nevertheless, these methods were initially formulated for mechanical loadings only. As soon as additional strains (thermal, swelling, shrinkage) are involved, some deviations might come. The aim of this contribution is to provide a method that allows to estimate the crack opening in concrete structures under various multi-physic loadings.

The study is divided into two parts. First, the damage mechanical modelling is presented and the crack opening routine is introduced. Second, applications are run: a rod is submitted to thermal and hydric loadings then a shear wall is studied under drying.

2 Concrete Crack Modelling

2.1 Mechanical Modelling

The mechanical model used in this work is an isotropic damage model; the decrease of the material stiffness is described by the evolution of a variable D ranging from 0 to 1. In an isotropic case, this scalar variable is introduced in the behaviour law "Eq. (1)".

$$\sigma = (1 - D)\mathbb{C} : \varepsilon \tag{1}$$

with $\mathbb{C}$ the four order stiffness tensor undamaged. The evolution of the damage depends on a load threshold function: $f = \varepsilon_{eq} - \kappa(D)$, where κ the hardening-softening parameter is equal to the maximum of ε_{eq} or ε_{d0} and ε_{d0} the tensile damage threshold corresponding to f_t/E. The equivalent strain (ε_{eq}) is taken as proposed by Mazars [4] and the evolution of damage in tension is taken as:

$$D = 1 - \frac{\epsilon_{d0}}{\epsilon_{eq}}\exp\left(-B_t\left(\epsilon_{eq} - \epsilon_{d0}\right)\right) \tag{2}$$

ϵ_{d0} (-) the damage threshold in tension and B_t, (-) the model parameters controlling the post-pic phase evolution of the material behaviour. To avoid mesh dependency and non-uniqueness of the solution due to softening behaviour of concrete, an energetic regularization is used [5, 6]. It is based on the parameter B_t (-) computed as a function of the size of element h (m), the tensile strength f_t (Pa), the fracture energy G_f (J.m^{-2}) and the threshold ϵ_{d0} (-):

$$B_t = \frac{h f_t}{G_f - \frac{h \epsilon_{d0} f_t}{2}} \tag{3}$$

2.2 Crack Opening Extraction Model

To compute the crack opening, let us assume that for a given time step i, the stress tensor, the scalar damage variable were computed. The post-processing method is composed of the following steps:

1. The total strain is computed with regard to the stress and the damage variable:

$$\varepsilon = [(1 - D)\mathbb{C}]^{-1} : \sigma \tag{4}$$

2. The elastic strain is computed according to the stress and the initial stiffness:

$$\varepsilon_e = [\mathbb{C}]^{-1} : \sigma \tag{5}$$

3. The anelastic strain is obtained combining Eqs. (4) and (5):

$$\varepsilon_{an} = \varepsilon - \varepsilon_e \tag{6}$$

4. Finally the crack opening is computed as follow with h_e the element size:

$$u_c = h_e \varepsilon_{an}. \tag{7}$$

3 Practical Case Studies

3.1 Rod Under Multi-physic Loadings

In the first application a rod under thermic and hygric loadings is modelled. The rod's dimensions are a length L of 0.20 m, a height of b of 0.02 m and each element size (h) are equal to 0.02. The modelling is carried out in 2D plane stress and is composed of 10 linear quadrangular elements. Regarding the boundaries conditions two cases scenario have to be distinguished. The first one models an imperfect rod submitted to free thermal expansion and drying shrinkage (Fig. 1a) and the second one simulates the same imperfect rod submitted to restrain thermal expansion and drying shrinkage (Fig. 1b). The model's parameters associated to the damage mechanical model are presented in the Table 1. In order to localize the damage and the related cracking, the sixth element is randomly introduced as a weak element with a strength value reduced by 50%. Thus, there is not regard according to regularization and B_t is adapted manually to the element size.

To model the thermal strains and the drying shrinkage a fictitious evolution is designed. The final strain related to drying shrinkage is chosen to be equal to 600 $\mu\epsilon$ and the thermal strains are designed to present a succession of levels (Fig. 2).

To validate the computed crack opening, the analytical value is calculated according to "Eq. (8)".

$$u_c = u_x - \frac{F_x}{E \times b}L - \sum_n \varepsilon_n \times L \tag{8}$$

with u_c (m) the analytical crack opening, u_x (m) the total axial displacement, F_x (N) the axial strength, E (Pa) the Young's modulus, b (m) the element height, L (m) the

Fig. 1 Two dimension rods with one imperfect element: Two cases scenario **a** free and **b** restrained
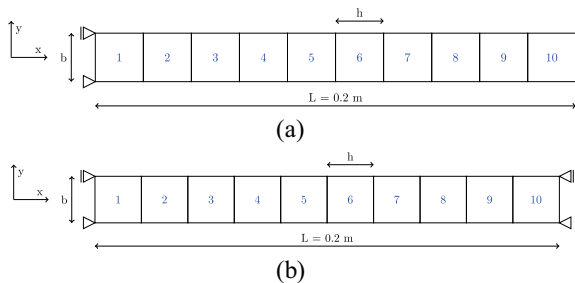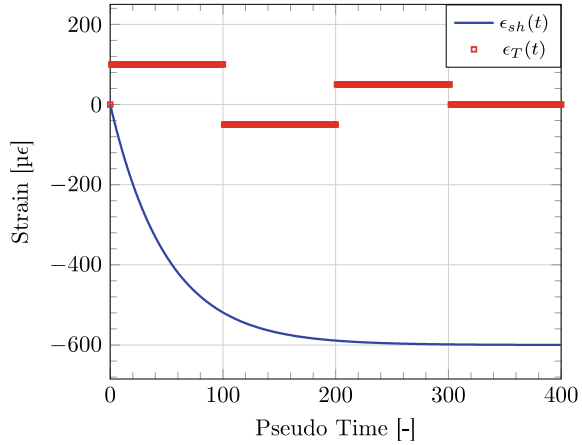

(a)

(b)

Table 1 Set of mechanical parameters of Mazars original model [4]

f_t (MPa)	E (GPa)	ν (-)	G_f (Jm^{-2})	Ac (-)	Bc (-)	At (-)	Bt (-)
3.0	30	0.2	300	1.4	1900	-20	0.01

Fig. 2 Designed imposed multi-physics strains

rod length and ε_n (-) the various additional strains. This analytical crack is computed according to numerical values.

The crack opening displacements computed in both scenario are plotted (Fig. 3). In the first modelling, the crack opening is expected to be equal to zero due to the free boundaries conditions. The theoretical value and the value computed with the proposed method are similar (no cracks) (Fig. 3a). However, the method published by Matallah et al. [2] found deviations from the analytical solution. The resulting cracks values are negative, which is not physical. Regarding the second modelling with restrained boundaries conditions (Fig. 3b), it is found that the proposed method meets the analytical value. As damage occurs, crack openings develop. There is a first stage where the rod is elastic then drying shrinkage and thermal expansion induced cracks. The final crack opening value is equal to 115.24 $\mu\varepsilon$ and 153 $\mu\varepsilon$ for the proposed method and the Matallah et al. [2] method respectively.
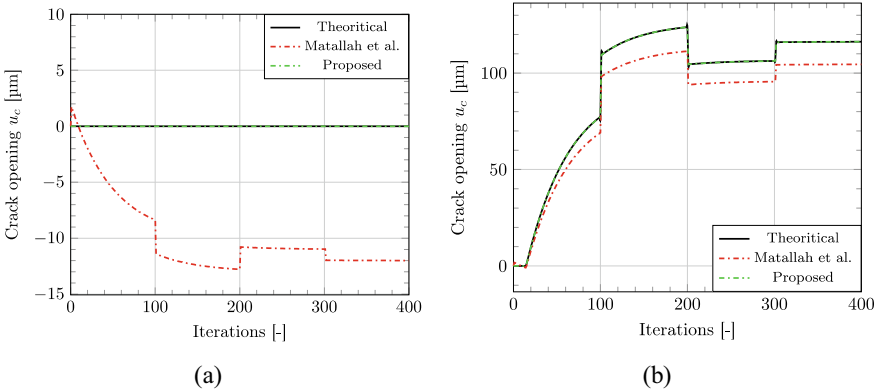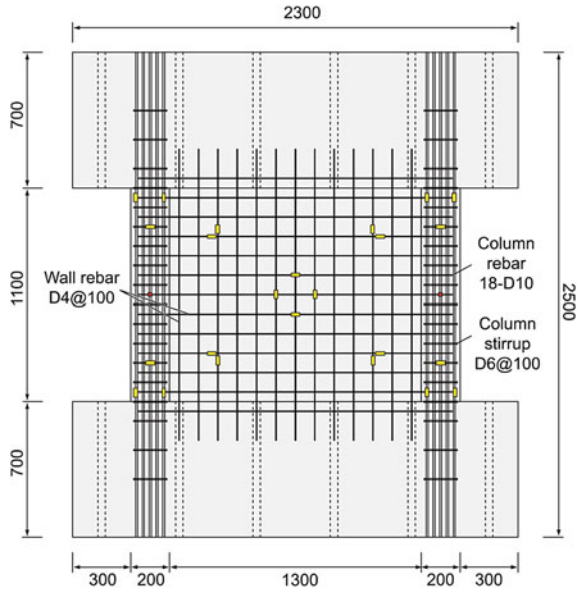

Fig. 3 Crack opening along the axial displacement: **a** free to deform and **b** restrained

Fig. 4 Schematic
representation of the shear
wall extracted from [7]

3.2 Shear Wall Under Drying

In this application, a semi-structural modelling of a shear wall submitted to drying
is undertaken. The modelling relies on the experimental investigation conducted by
Sasano et al. [7]. In this study two shear walls are exposed to a dried and sealed
environment for approximately 1 year. The ambient conditions regarding dry envi-
ronment is an average temperature and relative humidity of 18.4°C and 58.7% RH
respectively. The dimension of the wall are depicted on Fig. 4.

To model the ageing of the shear wall a previous model developed by the authors
is used [8]. It is composed of 4 main stages: the modelling of the drying process with
a diffusion equation including the capillary pressure as a driving potential "Eq. (9)".

$$\frac{dS_w}{dp_c}\frac{dp_c}{dt} = div(\frac{k_{rl}(S_w)K}{\mu_w\phi}grad(p_c)) \tag{9}$$

where S_w, p_c, ϕ, K, k_{rl} and μ_w are, respectively, the saturation degree, the capil-
lary pressure, the porosity, the intrinsic permeability, the relative permeability and
the viscosity of the liquid water. Saturation and relative permeability are computed
according to van Genuchten's relations [9]. Then the consideration of the drying
shrinkage "Eq. (10)":

$$\epsilon_{ds} = (1 - 2\nu)b_w S_w \int \left(\frac{1}{E}\frac{dp_c}{dt'} + J\left(t - t'\right)\frac{dp_c}{dt'}\right)dt' \tag{10}$$

with b_w (-) the Biot coefficient and J (Pa^{-1}) the creep compliance. Thus, the creep is considered according to "Eqs. (11)" and "(12)"

$$\frac{\dot{\sigma}}{k_{kv}} = \tau \varepsilon_{kv} + \left(1 + \frac{\dot{k}_{kv}}{k_{kv}}\right)\dot{\varepsilon}_{kv} \text{ and } \sigma = \eta_{am}\dot{\varepsilon}_{am} \text{ with } \dot{\varepsilon} = \dot{\varepsilon}_{kv} + \dot{\varepsilon}_{am} \quad (11)$$

$$\dot{\epsilon}_{dc} = \lambda_{dc}|\dot{\epsilon}_{ds}|\sigma \quad (12)$$

where k_{kv} (Pa), τ (s), η_{am} (Pa.s) and λ_{dc} (-) are material parameters and a constant respectively. Creep is extended to multiaxial state of stress thank to the creep Poisson ratio. The mechanical model (presented in Sect. 2.1) is slightly modified to consider the pore pressure which will strengthen the material according to desaturation "Eq. (13)".

$$\sigma = (1 - D)\,\tilde{\sigma} + b_m S_w p_c \mathbf{1} \text{ with } \dot{\tilde{\sigma}} = \mathbb{C} : (\dot{\epsilon} - \dot{\epsilon}_c - \dot{\epsilon}_{ds}) \quad (13)$$

with $\tilde{\sigma}$ the effective stress, b_m a material parameter and $\mathbf{1}$ the unit tensor. Finally, to model the ageing of shear wall, the identification of the model parameter has to be done. There were informations regarding drying, drying shrinkage and mechanical parameters in Sasano et al. [7] work. However, there was no consideration of creep. To overcome this limit an assumption on creep parameters was done (parameters taken from another identification on a concrete close to the one used in Sasano study). The identified parameters are gathered in the Tables 2, 3 and 4. Regarding mechanical parameters, it is assumed that damage in compression never occurs. As a result compressive damage parameters are unused. Moreover, an energetic regularization is introduced according to "Eq. (3)" in order to prevent mesh dependency.

Table 2 Set of drying parameters identified on Sasano et al. [7] experimental tests

β (-)	α (-)	n_k (-)	K_{int} (m^2)	φ (-)	ρ (kg.m^{-3})
0.48	13	−0.23	6.4. 10−21	0.143	2365

Table 3 Set of creep parameters extracted from [8]

τ_{am} (d)	η_∞ (GPa.s)	k_{kv} (GPa)	τ_{kv} (d)	ν_{bc} (-)	λ_{dc} (MPa^{-1})
90	130	135	15	0.1	7.82. 10^{-2}

Table 4 Identified mechanical parameters for the shear wall under drying

f_t (MPa)	E (GPa)	ν (-)	G_f (Jm^{-2})	At (-)	b_m (-)
3.1	30.4	0.23	100	0	0.01

(a)   (b)
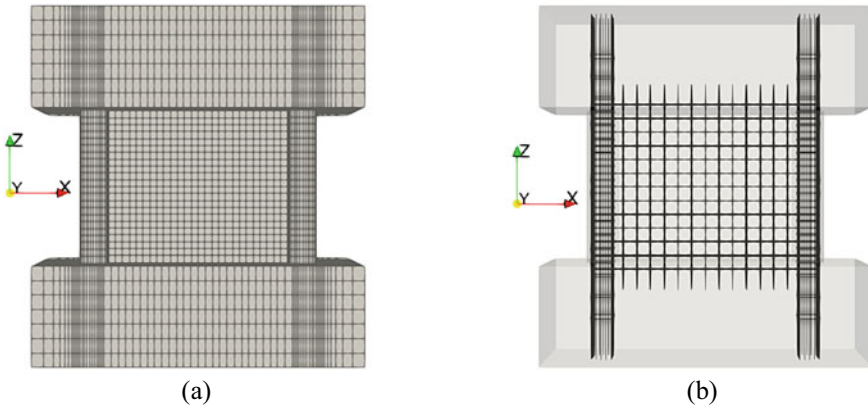
Fig. 5 Modelling of the RC wall specimen **a** 3 dimensional modelling and **b** modelled rebar reinforcements

The shear wall is modelled using a 3 dimensional modelling. The mesh is composed of 35576 cubic elements and 3644 linear elements with a linear formulation (Fig. 5a and b). Rebar reinforcements and volumetric element are linked with a kinematic relationship that imposes a perfect adhesion. Moreover the boundaries conditions are implemented to block the symmetry axes allowing a free deformation. As a first attempt, a random field on the tensile strength is generated using the Turning Band Method [10]. A coefficient of variation equal to 10% and a correlation length equal to three times the biggest aggregate (15 mm) are considered.

For a sake of clarity, the results of this study focus only on crack openings. However, in order to highlight the hydro-mechanical modelling some insights on the relative humidity fields resulting of one year of drying and on the mechanical variable are given such as damage and the crack openings.

Thus, Fig. 6 shows the distribution of the relative humidity fields after 372 days of drying. One can note that the wall reached the equilibrium state ($h_r = 58.7\%$). However, it is not the case concerning the columns and the stubs. These are close to 75% and 100% relative humidity in the core respectively. As a result in addition to the rebar reinforcement, these elements will prevent the shrinkage of the wall and favor cracks at the interface between the wall and them.

Concerning mechanical results, Fig. 7a draws the damage variable. This variable is mainly concentrated superficially on the edges of the structure. The stubs are the most damaged parts of the structure. If one focus on the wall, the damage variable does not exceed the value of 0.45. It is noticeable that damage concentration are occurring on the corner of the wall. One of this concentration goes through the wall. Then, the post-processing technic is applied. The results are depicted on Fig. 7b. The crack opening field induced by drying shrinkage is very similar to the damage field. A concentration of cracks is found on the stubs. The crack openings are in the range of 100 μm with the biggest value equal to 150 μm. One can note that the crack
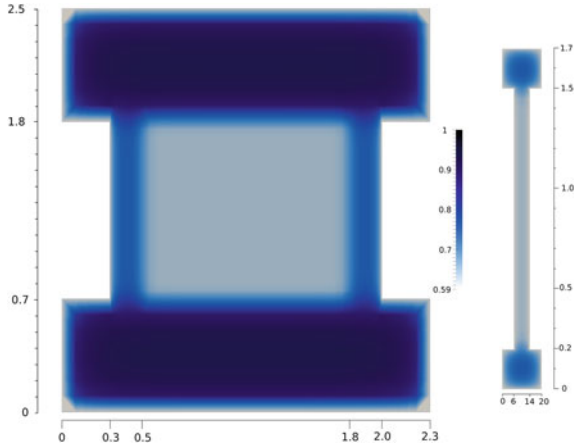
Fig. 6 Relative humidity field after 372 days of drying. (Left) Cross section at the middle of the depth, (right) Cross section at the middle of the height
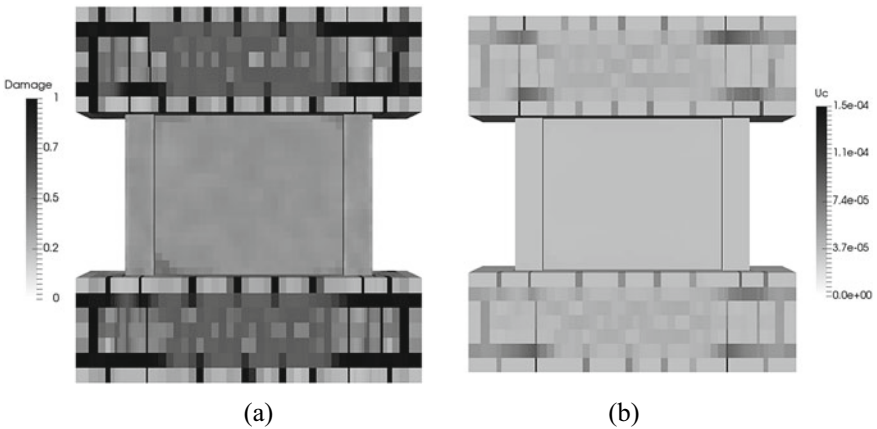

(a)   (b)

Fig. 7 Computed mechanical fields after 372 days: **a** Damage and **b** crack openings in meter

openings found in the wall are much smaller than that. They are invisible at with the range scale used in Fig. 7.

Figure 8 highlights the cracks on the wall. Monitored cracks are placed in front of computed cracks. These experimental cracks openings ranged from a few tenth of micrometer to 150 μm. Corresponding numerical openings are close to few micrometer. Wide deviations between them exist. This is probably due to both the assumption on the identified parameters (creep for instance) and the modelling hypothesis. Indeed, perfect adhesion between concrete and rebar leads to a slight overestimation of the structure behaviour. As the interface between both materials is perfect there is no slippage and the resulting behaviour is stiffer. Regarding the localization
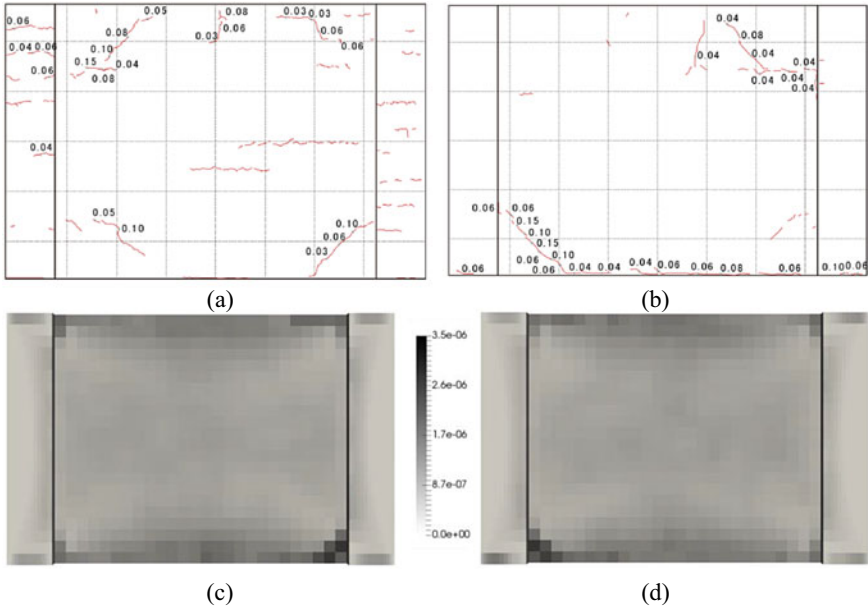
(a) (b) (c) (d)

Fig. 8 Experimental and numerical crack opening induced by drying shrinkage at the end of drying (372 days) **a** Face 1 **b** Face 2 **c** Numerical Face 1 and **d** Face 2. Crack opening measured in mm for experimental results and in meter in modelling

of cracks, computed values found agreements with experimental findings. Diagonal cracks at four corners of the wall are partially reproduced and cracks at the interface between stubs and wall are captured. Conversely, it is harder to model the cracks on the columns. These are controlled by material variability, damage model parameters and steel-concrete binding assumptions.

4 Conclusion

Crack is an important feature of concrete material. Often model with damage approach, crack is not explicitly available. Post-processing methods were developed to overcome this limit and roughly estimate the crack openings. They were designed to consider only cracks induced by mechanical loadings.

To extend these methods to multi-physics loadings, a post processing routine was developed. It was tested on academical tests and compared to the analytical solutions. This step yielded satisfactory results. Further investigations were undertaken with a semi-structural application based on Sasano et al. work. With the use of a chained hydro-mechanical modelling, cracks induced by drying were characterized.

The routine managed to locate the area where cracks developed but partially due to model assumptions the cracks openings were slightly underestimated.

The proposed method is thus a good alternative to sophisticated approaches to capture cracks in large structures.

References

1. Bottoni, M., Dufour, F., Giry, C.: Topological search of the crack pattern from a continuum mechanical computation. Eng. Struct. **99**, 346–359 (2015)
2. Matallah, M., La Borderie, C., Maurel, O.: A practical method to estimate crack openings in concrete structures. Int. J. Numer. Anal. Meth. Geomech. **34**, 1615–1633 (2010)
3. Dufour, F., Pijaudier-Cabot, G., Choinska, M., Huerta, A.: Extraction of a crack opening from a continuous approach using regularized damage models. Computers and Concrete **5**, 375–388 (2008)
4. Mazars, J.: A description of micro- and macroscale damage of concrete structures. Eng. Fract. Mech. **25**, 729–737 (1986)
5. Bazant, Z.P., Oh, B.H.: Crack band theory for fracture of concrete. Mater. Struct. **16**, 155–177 (1983)
6. Hillerborg, A., Modéer, M., Petersson, P.-E.: Analysis of crack formation and crack growth in concrete by means of fracture mechanics and finite elements. Cem. Concr. Res. **6**, 773–782 (1976)
7. Sasano, H., Maruyama, I., Nakamura, A., Yamamoto, Y., Teshigawara, M.: Impact of drying on structural performance of reinforced concrete shear walls. J. Adv. Concr. Technol. **16**, 210–232 (2018)
8. Soleilhet, F., Benboudjema, F., Jourdain, X., Gatuingt, F.: Role of pore pressure on cracking and mechanical performance of concrete subjected to drying. Cem. Concr. Compos. **114**(103727) (2020)
9. Van Genuchten, M.T., Nielsen, D.: On describing and predicting the hydraulic properties. Ann. Geophys. **3**(5), 615–628 (1985)
10. Matheron G.: The intrinsic random functions and their applications. Adv. Appl. Probab. 439–468 (1973)